Cross sections in the $^{59}Co(n,n'\gamma)$ ^{59}Co reaction from 1.1 to 3.3 MeV

R. V. LeClaire,* J. J. Egan, L. E. Beghian, G. P. Couchell, G. H. R. Kegel, S. C. Mathur, A. Mittler, and W. A. Schier

University of Lowell, Lowell, Massachusetts 01854

(Received 14 September 1977; revised manuscript received 15 March 1978)

The $^{59}Co(n,n'\gamma)$ ^{59}Co reaction was employed to obtain neutron inelastic scattering cross sections for nineteen levels in ^{59}Co in the incident neutron energy range 1.11 to 3.32 MeV. These cross sections were deduced from measured γ-ray production cross sections for thirty-six γ rays observed in the decay of ^{59}Co using a 40 cm^3Ge (Li) detector. Branching ratios have been determined for forty transitions from levels up to 3016 keV. The pulsed-beam time-of-flight technique was employed for background reduction. The data were corrected for neutron multiple scattering and neutron and γ-ray attenuation effects. The neutron inelastic scattering cross section data for the nineteen levels are compared to compound nucleus statistical model calculations. On the basis of these calculations and the branching ratios previously assigned spins for states up to 2062 keV have been confirmed. Spin assignments are made for the following states: 2087 keV(5/2 or 7/2), 2153(11/2 or 13/2), 2183(5/2, 7/2, or 9/2), 2206(3/2, 5/2, or 7/2), 2395(7/2, 9/2, or 11/2), 2479(3/2, 5/2, or 7/2), 2542(3/2, 5/2, or 7/2), 2585(7/2 or 9/2), 2713(1/2 or 3/2), 2781(3/2 or 5/2), 2824(3/2–9/2), and 2962 keV(3/2, 5/2, or 7/2).

[NUCLEAR REACTIONS $^{59}Co(n,n'\gamma)$, E_n = 1.1–3.3 MeV; measured $\sigma(E;E_\gamma,\theta)$. Deduced $^{59}Co(n,n')$ cross sections, ^{59}Co decay scheme, J, γ-decay branching ratios.]

I. INTRODUCTION

This work was undertaken as part of an effort to establish accurate neutron inelastic scattering cross sections in the $A = 46$ to 60 mass region for neutrons up to 3.5 MeV in energy. The elements in this mass region include the principal constituents of ferrous alloys which are used as structural materials in reactors and other installations where fast neutrons abound.

In addition to their significance in the neutron slowing down process in structural materials cobalt inelastic scattering cross sections are useful in the establishment of a consistent set of reaction model parameters in the $A = 40$–60 mass region. Such parameters can be used in theoretical calculations to extend the currently available cross-section information to energy regions, and to neighboring nuclei, where measurements have not been performed.

The energy level and decay scheme of ^{59}Co are also of interest from a basic physics point of view. The structure of the ^{59}Co nucleus lends itself to interpretation via the unified vibrational model with the single-hole proton configuration $(f_{7/2})^{-1}$ coupled to a quadrupole vibrational ^{60}Ni core. Spectroscopic information obtained in this work is compared to the predictions of these model calculations.

The most accurate ^{59}Co inelastic cross-section information previously available has been obtained from (n,n') measurements by Guenther *et al.*[1] Their work forms the basis of the ENDF/B-IV evaluation[2] for inelastic neutron scattering from cobalt. This evaluation was based solely on (n,n') measurements because, as Ref. 1 points out, previous $(n,n'\gamma)$ studies[3-6] yielded inconsistent results which were difficult to interpret.

The earliest $(n,n'\gamma)$ work[3] on cobalt was done before the advent of Ge(Li) detectors. The $(n,n'\gamma)$ work at Texas Nuclear Corporation[4] does not agree well at all with the (n,n') measurements even for states which are well resolved in the neutron spectra. Broder *et al.*[5] only reported γ-ray production cross sections for four transitions. Daniels and Felsteiner[6] reported relative γ-production rates at 2.9 MeV and assigned spins to several levels.

In the present work we observed forty γ-ray transitions following inelastic scattering of neutrons from ^{59}Co. From the measurements we have established the energy level and decay scheme of ^{59}Co. We have determined the γ-ray production cross sections for thirty-six transitions, and from these we have deduced the neutron inelastic scattering cross sections for nineteen levels. γ-ray branching ratios have been determined for levels up to 3016 keV.

A set of optical model parameters has been obtained by comparing available elastic scattering data to optical model calculations. The inelastic scattering data were then compared to theoretical Hauser-Feshbach statistical model[7] calculations for states whose spins and parities were previous-

ly established, providing a check on the reliability of the calculations. The transmission coefficients for the statistical model calculations were generated in an optical model code which employed the parameters obtained in the analysis of the elastic scattering data. Thus the inelastic scattering calculations are dependent upon the optical parameters, and comparison with the inelastic data is useful in establishing a consistent set of such parameters. Further calculations for states of unknown spin along with information obtained from the branching ratio measurements enable us to make spin assignments for twelve levels between 2 and 3 MeV in excitation, a region where only minimal spectroscopic information, other than energy level values, previously existed.

II. EXPERIMENTAL PROCEDURE

Because of its excellent energy resolution, the $(n,n'\gamma)$ technique is particularly well suited for cross-section studies in the 1–3 MeV region on medium mass nuclei. In these nuclei the levels above 1 MeV in excitation are rather closely spaced. In addition the internal conversion coefficients for electromagnetic transitions are very small and the γ-ray yields are appreciable. The alternative (n,n') technique, using time of flight, is beset by resolution problems which can be overcome to some extent by using long flight paths resulting in very low count rates. Recent time-of-flight (n,n') measurements[8] have been made at the University of Lowell with very high resolution (~22 keV) using three-meter flight paths, but these necessarily entail long running times and are applicable when only small regions in excitation (~400 keV wide) are being examined. These latter experiments are specifically designed for investigations in the 1–3 MeV bombarding energy range on the low-lying levels of the heavy elements where severe γ-ray attenuation and large internal-conversion coefficients preclude γ-ray measurements.

In the present experiment the scattering sample consisted of a right circular cylinder, 2.54 cm in diameter by 5.00 cm in height, containing 2.85 moles of elemental cobalt. A 40-cm^3 Ge(Li) crystal was employed to detect the γ rays. Figure 1 depicts the experimental arrangement.

The University of Lowell 5.5-MV Van de Graaff generator, operating in a pulsed mode, produced proton bursts of approximately 5 nsec duration at a 5-MHz rate. Neutrons were generated via the ^{3}H$(p,n)^3$He reaction. The tritium target consisted of a platinum disk containing a thin titanium deposit into which the tritium was absorbed. The total amount of tritium absorbed was approximately 4 Ci resulting in a target thickness that varied from 95 keV for 2.0-MeV protons to 55 keV for 4.5-MeV protons.

In order to minimize background γ rays in the energy spectra, the Ge(Li) detector was surrounded by lead rings, which were imbedded in a lithium carbonate and paraffin shield. A copper shadow bar was positioned in such a way as to protect the crystal from direct target neutrons. The entire detector-shielding arrangement was placed on a goniometer enabling angular distribution measurements to be taken back to 135°.

To further suppress background γ rays a time-of-flight (TOF) system was employed. Time-gating of the Ge(Li) energy spectrum reduced the intensity of most background γ rays by about 80%. Also a NaI(Tl) anti-Compton annulus was used in the initial phases of the experiment. The additional background suppression provided by the anti-

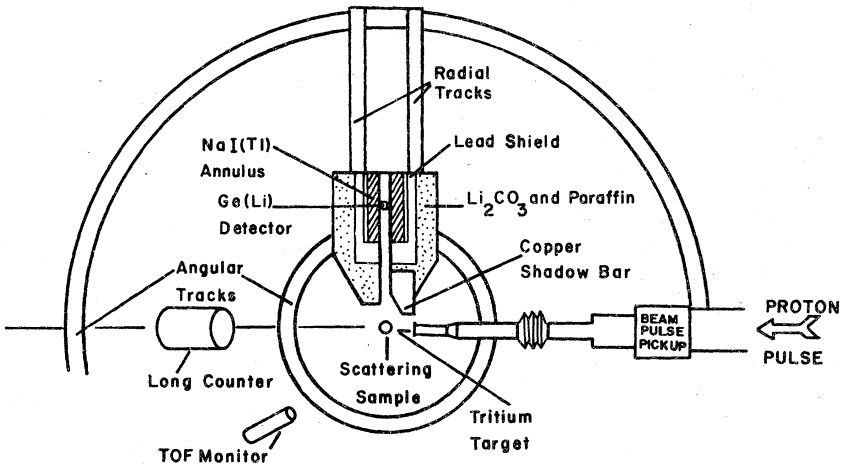

FIG. 1. Experimental arrangement in the target room for the time-gated-γ-ray measurements in the ^{59}Co$(n,n'\gamma)$ reaction.

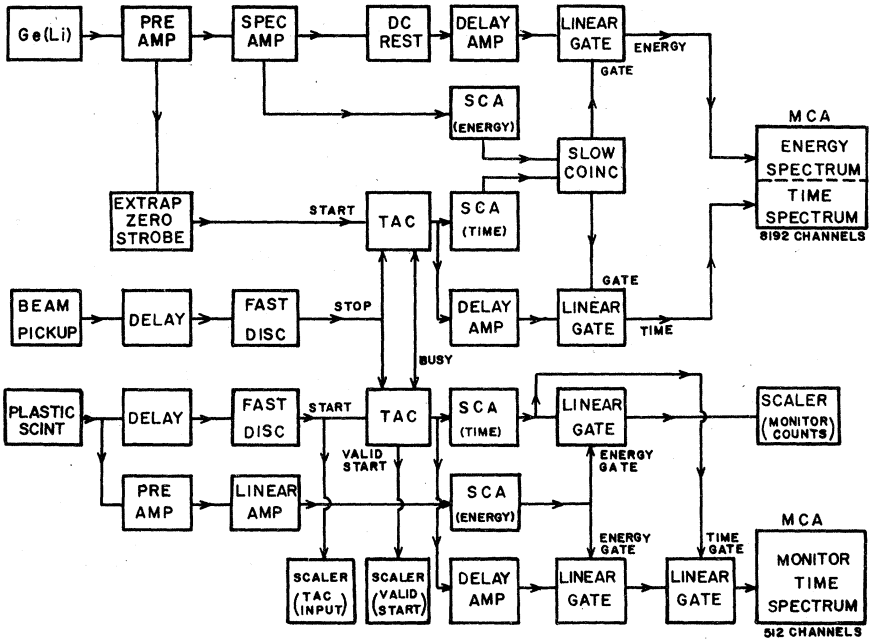

FIG. 2. Electronics block diagram for Ge(Li) and plastic scintillator time-of-flight detector systems.

Compton annulus was useful when we were trying to establish the decay scheme. However, it was necessary to remove the annulus from the system during the cross-section measurements because neutron activation of the sodium iodide led to unacceptably high count rates in the annulus and hence to the accidental rejection of a large fraction of the Ge(Li) full-energy signals.

The block diagram of the electronic system employed is shown in Fig. 2. The plastic scintillator detection system is described below. The anti-Compton annulus is not included but its addition simply introduces another signal in anticoincidence at the slow coincidence unit. A time-of-flight spectrum for this system taken with an iron scattering sample is shown in Fig. 3. The flight path was 0.92 m and the full width at half maximum of the γ-ray peak was 5.9 nsec. Figure 4 shows a γ-ray spectrum for ^{59}Co using this system with the anti-Compton NaI(Tl) annulus in place.

The neutron fluence was monitored with a Hansen-McKibben[9] long counter located at zero degrees to the incident beam direction. For neutron energies above 2 MeV the long counter was calibrated on an absolute scale against a proton recoil telescope of the Los Alamos design[10] as described by Johnson.[11] The proton detector was a surface barrier detector rather than the scintillation device described in Ref. 11.

For energies below 2 MeV, where the response of the recoil telescope was too poor for accurate measurements, a relative calibration of the long counter was accomplished by comparison to the known $^{3}H(p,n)^{3}He$ cross section. Sufficient overlap points between the recoil telescope and the $^{3}H(p,n)^{3}He$ measurements were taken in order to normalize the relative calibration to the absolute.

Since the long counter was placed at zero degrees, the incident fluence could not be measured with the scattering sample in place. Consequently after each Ge(Li) detector measurement was made the zero-degree fluence was determined by acquiring long counter data with the scattering sample

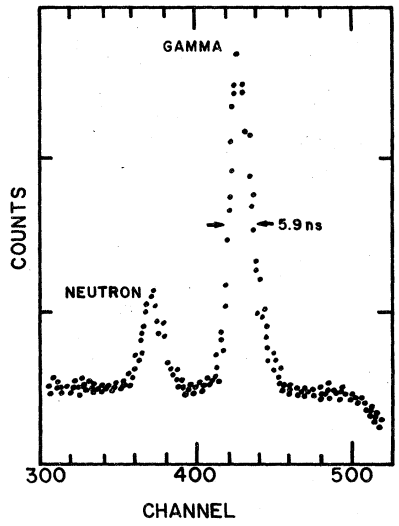

FIG. 3. A Ge(Li) time-of-flight spectrum using the system depicted in Figs. 1 and 2 for an iron scatterer.

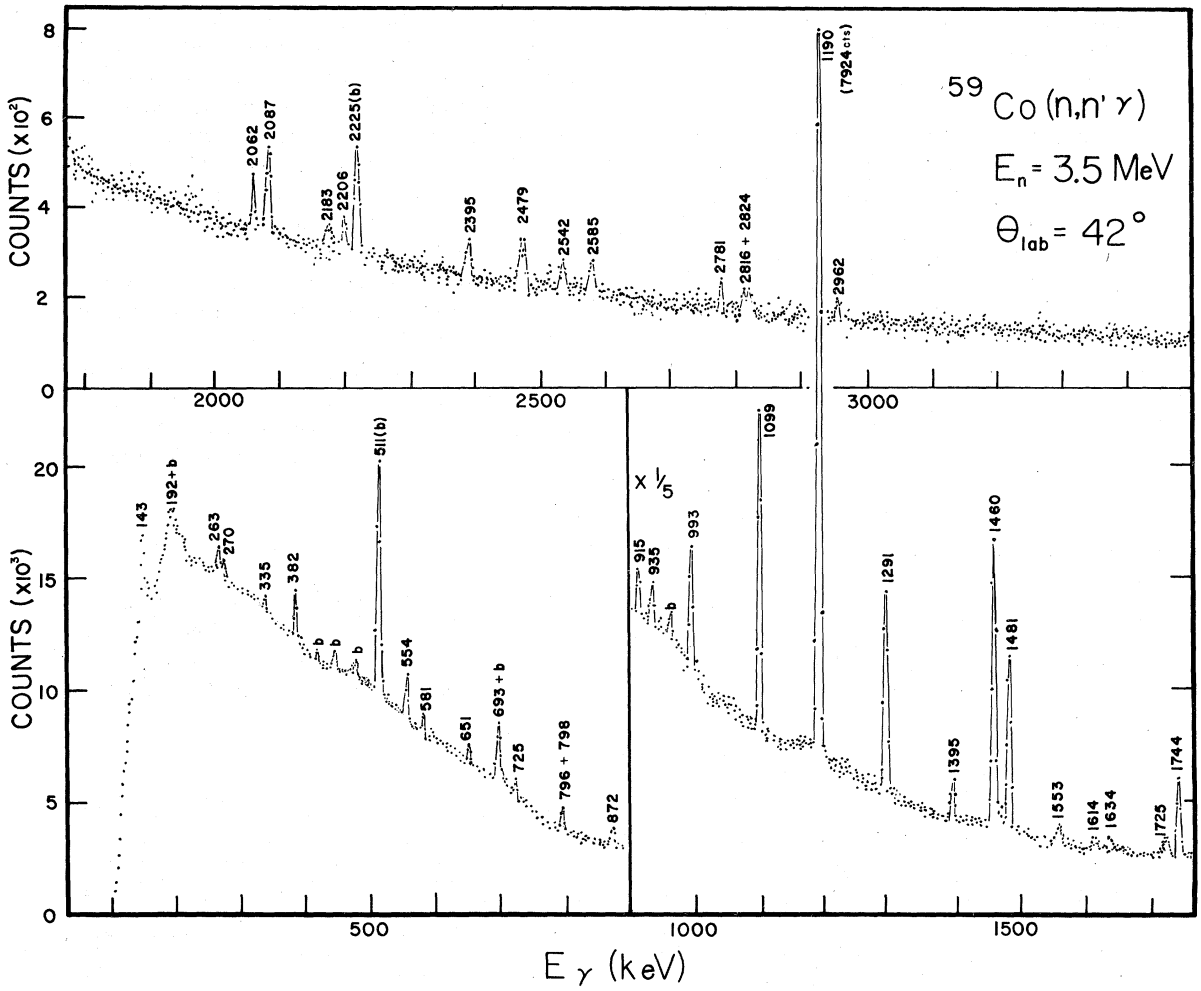

FIG. 4. ^{59}Co γ-ray spectrum at E_n = 3.5 MeV using the anti-Compton annulus.

removed. The normalization of these runs was accomplished by a second time-of-flight system employing a plastic scintillator mounted on a photomultiplier tube. This detector was placed in such a way as to have an unobstructed path to the tritium target at all times. It was also used for the normalization of the long counter calibration measurements performed with the recoil telescope. The electronics arrangement for this detector is included in Fig. 2.

The product of the efficiency of the Ge(Li) detector by the solid angle it subtends at the sample (a quantity needed in the determination of the cross section from the data) was obtained by using standard γ-ray sources of known intensity placed at the position of the scattering sample. The time-of-flight electronics were used in these efficiency measurements by deriving a time-to-amplitude converter (TAC) stop pulse from a delayed output of the extrapolated zero strobe, thereby taking into account the effect of the complete electronic system on the efficiency.

III. DATA REDUCTION

The γ-ray production cross sections σ_γ were calculated from the expression

$$\sigma_\gamma(\theta) = \frac{Y_c(\theta)}{FN\epsilon\Delta\Omega},$$

where

$Y_c(\theta)$ is the yield under a full-energy peak in the γ spectrum corrected for neutron multiple scattering and neutron and γ attenuation;

$\epsilon\Delta\Omega$ is the product of the γ-ray full-energy peak efficiency and the solid angle subtended by the detector;

F is the neutron fluence in the sample as determined from the long counter and recoil telescope calibration measurements; and N is the number of cobalt atoms in the sample.

The γ-ray yields were obtained using the peak fitting and area extraction code, GASPAN.[12] The multiple scattering corrections were calculated using parameters obtained from Kinney.[13] Employing Monte Carlo calculations he showed that the multiple scattering corrections depend only on the height-to-diameter ratio of the sample. A code, ABBSIG,[14] was written at our laboratory which accounted for neutron multiple scattering as well as neutron and γ-ray attenuation effects.

The fluence in the sample, F in the equation above, was determined taking into account the anisotropic angular distribution of the neutrons impinging on the sample. The multiple scattering and attenuation effects also depend upon the angular distribution of the incident neutrons and this was accounted for in ABSSIG.

The full-energy peak efficiency of the Ge(Li) detector was determined using calibrated sources. Since the efficiency nearly obeys a power law in dependence on γ-ray energy, the efficiency data vs. energy on a log-log plot yields a linear dependence which is easily fitted by a least squares procedure.

The uncertainties in the determination of the foregoing quantities were combined to give the absolute errors presented in the results below. The errors in the extraction of the areas of the full-energy peak, including statistical errors, ranged from 5% for strong isolated γ-ray peaks, to 30% for some of the very weak transitions and for the 693-keV transition which is partially obscured by a background line. The uncertainty in the absolute zero-degree neutron fluence was 6%. The uncertainty in the Ge(Li) detector efficiency was 4%. The uncertainties in the cross sections due to the finite sample corrections, and to the correction for the variation of the neutron fluence through the sample, were estimated to vary from 1.5% for high energy transitions to 5% for low energy transitions.

IV. RESULTS

The ^{59}Co level and decay scheme obtained in this experiment is shown in Fig. 5. The transitions of energies 935, 1553, 1634, 2183, and 2542 keV have not been observed previously. Table I sum-

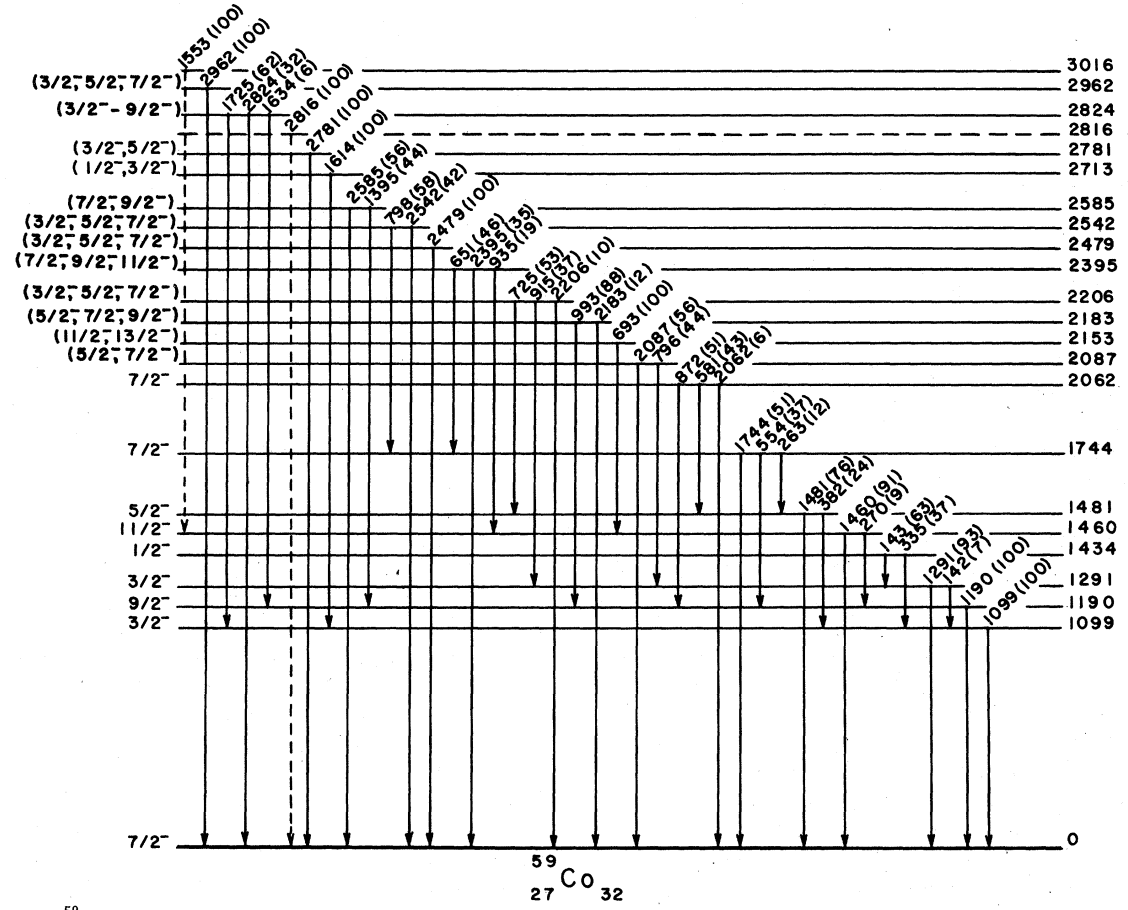

FIG. 5. ^{59}Co level and decay scheme. Spins for states above 2062 keV are based upon the results of this experiment.

TABLE I. Level energies, γ-ray energies, spins, and branching ratios determined in the present experiment. The J^π values up to and including the 2062-keV state had been previously established and are confirmed here. *A* comparison is made with the branching ratios of Coop *et al.* (Ref. 15).

Initial state (keV)	Assigned J_i^π	Best fit J_i^π	Final state (keV)	J_f^π	E_γ (keV)	Branching ratio (%) Present work	Coop *et al.* (Ref. 15)
1099	$\frac{3}{2}^-$	$\frac{3}{2}^-$	0	$\frac{7}{2}^-$	1099	100	100
1190	$\frac{9}{2}^-$	$\frac{9}{2}^-$	0	$\frac{7}{2}^-$	1190	100	100
1291	$\frac{3}{2}^-$	$\frac{3}{2}^-$	0	$\frac{7}{2}^-$	1291	93 ± 2	93 ± 4
			1099	$\frac{3}{2}^-$	192	7 ± 2	7 ± 4
1434	$\frac{1}{2}^-$	$\frac{1}{2}^-$	1099	$\frac{3}{2}^-$	335	37 ± 4	···
			1291	$\frac{3}{2}^-$	143	63 ± 4	···
1460	$\frac{11}{2}^-$	$\frac{11}{2}^-$	0	$\frac{7}{2}^-$	1460	91 ± 1	>90
			1190	$\frac{9}{2}^-$	270	9 ± 1	<10
1481	$\frac{5}{2}^-$	$\frac{5}{2}^-$	0	$\frac{7}{2}^-$	1481	76 ± 2	80 ± 3
			1099	$\frac{3}{2}^-$	382	24 ± 3	20 ± 3
1744	$\frac{7}{2}^-$	$\frac{7}{2}^-$	0	$\frac{7}{2}^-$	1744	51 ± 2	59 ± 3
			1190	$\frac{9}{2}^-$	554	37 ± 2	32 ± 2
			1481	$\frac{5}{2}^-$	263	12 ± 2	9 ± 2
2062	$\frac{7}{2}^-$	$\frac{7}{2}^-$	0	$\frac{7}{2}^-$	2062	6 ± 2	weak
			1190	$\frac{9}{2}^-$	872	51 ± 3	weak
			1481	$\frac{5}{2}^-$	581	43 ± 3	strong
2087	$(\frac{5}{2}^-, \frac{7}{2}^-)$	$\frac{5}{2}^-$	0	$\frac{7}{2}^-$	2087	56 ± 6	weak
			1291	$\frac{3}{2}^-$	796	44 ± 6	weak
2153	$(\frac{11}{2}^-, \frac{13}{2}^-)$	$\frac{13}{2}^-$	1460	$\frac{11}{2}^-$	693	100	···
2183	$(\frac{5}{2}^-, \frac{7}{2}^-, \frac{9}{2}^-)$	$\frac{7}{2}^-$	0	$\frac{7}{2}^-$	2183	12 ± 4	···
			1190	$\frac{9}{2}^-$	993	88 ± 4	weak
2206	$(\frac{3}{2}^-, \frac{5}{2}^-, \frac{7}{2}^-)$	$\frac{5}{2}^-$	0	$\frac{7}{2}^-$	2206	10 ± 6	···
			1291	$\frac{3}{2}^-$	915	37 ± 6	···
			1481	$\frac{5}{2}^-$	725	53 ± 6	···
2395	$(\frac{7}{2}^-, \frac{9}{2}^-, \frac{11}{2}^-)$	$\frac{9}{2}^-$	0	$\frac{7}{2}^-$	2395	35 ± 3	18 ± 9
			1460	$\frac{11}{2}^-$	935	19 ± 3	···
			1744	$\frac{7}{2}^-$	651	46 ± 3	22 ± 6
2479	$(\frac{3}{2}^-, \frac{5}{2}^-, \frac{7}{2}^-)$	$\frac{5}{2}^-$	0	$\frac{7}{2}^-$	2479	100	>90
2542	$(\frac{3}{2}^-, \frac{5}{2}^-, \frac{7}{2}^-)$	$\frac{5}{2}^-$	0	$\frac{7}{2}^-$	2542	42 ± 3	···
			1744	$\frac{7}{2}^-$	798	58 ± 3	>80
2585	$(\frac{7}{2}^-, \frac{9}{2}^-)$	$\frac{9}{2}^-$	0	$\frac{7}{2}^-$	2585	56 ± 8	60 ± 8
			1190	$\frac{9}{2}^-$	1395	44 ± 8	40 ± 8
2713	$(\frac{1}{2}^-, \frac{3}{2}^-)$	···	1099	$\frac{3}{2}^-$	1614	100	···
2781	$(\frac{3}{2}^-, \frac{5}{2}^-)$	$\frac{3}{2}^-$	0	$\frac{7}{2}^-$	2781	100	···
2816	···	···	0	$\frac{7}{2}^-$	2816	100	···

TABLE I. *(Continued)*.

Initial state (keV)	Assigned J_i^π	Best fit J_i^π	Final state (keV)	J_f^π	E_γ (keV)	Branching ratio (%) Present work	Coop *et al.* (Ref. 15)
2824	$(\frac{3}{2}^- - \frac{9}{2}^-)$	$\frac{9}{2}^-$	0	$\frac{7}{2}^-$	2824	32 ± 15	···
			1099	$\frac{5}{2}^-$	1725	62 ± 15	···
			1190	$\frac{9}{2}^-$	1634	6 ± 2	···
2962	$(\frac{3}{2}^-, \frac{5}{2}^-, \frac{7}{2}^-)$	$\frac{3}{2}^-, \frac{5}{2}^-$	0	$\frac{7}{2}^-$	2962	100	···
3016	···	···	1460	$\frac{11}{2}^-$	1553	100	···

marizes the γ transitions and their branching ratios determined in this experiment. For comparison the branching ratios of Coop *et al.*[15] are also included. The energy values for the levels in Fig. 5 are similar to those listed in the Nuclear Data Sheets[16] up to 2.3 MeV and agree closely with the recent work of Mateja *et al.*[17] Above 2.3 MeV our energies differ from those reported in Ref. 16 but agree generally with those of Ref. 17. Twenty-five of the forty γ transitions observed here have been reported by Brondi *et al.*[18] They did not observe the five new transitions mentioned above, the 270-, 651-, 872-, 798-, 993-, and 1395-keV transitions which were reported in Ref. 15 and the 143-, 192-, 693-, and 2395-keV transitions which are included in the Nuclear Data Sheets. The spin assignments indicated in Fig. 5 and Table I are consistent with the branching ratios and with the comparison to theoretical calculations discussed below.

γ-ray excitation functions were measured at 90° and 125° from 1.11 to 3.32 MeV. γ-ray angular distributions for the stronger transitions were measured at 1.41, 1.76, 1.91, 2.32, and 2.82 MeV. Figures 6 and 7 show the integrated γ-ray production cross sections for thirty-six γ-ray transitions. Figures 8 and 9 contain representative γ-ray angular distributions at 1.76 and 2.82 MeV respectively. The solid curves in Figs. 8 and 9 represent Legendre polynomial fits to the data.

The integral γ-ray production cross sections were obtained by fitting each of the angular distributions with a series of Legendre polynomials. This provided accurate cross sections for those bombarding energies and transitions for which complete angular distributions were available. At energies other than the five mentioned above and for the weaker transitions the 125° excitation function data were used in obtaining the integrated cross sections. The 90° excitation function data were useful as a check on the shape of the angular distributions.

Angular distribution data were obtained for three transitions at $E_n = 1.41$ MeV, for eight transitions at 1.76 MeV, for five transitions at 1.91 MeV, for twelve transitions at 2.32 MeV, and for sixteen transitions at 2.82 MeV. Only one of these forty-four cases required a term beyond second order in the Legendre polynomial fits to the data. This one case which required a small fourth order term was peculiar, however, in that it was an angular distribution for the sum of the 796- and 798-keV transitions taken at 2.82 MeV.

It is customary to obtain integrated γ-ray production cross sections from the 125° γ-ray data. This angle corresponds to a zero of P_2, the Legendre polynomial of the second order. In a series expansion,

$$\frac{d\sigma}{d\Omega} = \sum_n a_n P_n ,$$

the coefficients of all odd-order polynomials are zero because of the theoretically expected and experimentally substantiated symmetry of the angular distributions about 90°. When measurements are made at 125° the cross section can be written

$$\frac{d\sigma}{d\Omega}(125°) \cong a_0 + a_4 P_4 + \cdots .$$

If the angular distribution measurements indicate no P_4 or higher contributions, we have simply

$$\sigma = \int \frac{d\sigma}{d\Omega} d\Omega = a_0 \int d\Omega = 4\pi a_0 = 4\pi \frac{d\sigma}{d\Omega}(125°) ,$$

where σ is the desired integrated cross section.

Since it was possible to fit all but one angular distribution, and that was a special case, with only P_0 and P_2 contributions it is reasonable to assume that within the accuracy of the data for the strong transitions there are no significant P_4 contributions at energies where angular distributions were not made. Further we have ignored P_4 contributions for the weaker transitions where the statistical errors are fairly large and for which we have no angular distributions. Hence the

integrated γ-ray production cross sections shown in Figs. 6 and 7 correspond to 4π times the 125° data.

The angular distribution and excitation function data were completely independent measurements. In eighty percent of the cases (28 out of 35) where it was possible to compare $4\pi a_0$ from the angular distribution data to $4\pi\sigma(125°)$ from the excitation function measurements the two values agreed within experimental accuracy. In other cases the two numbers differed by as much as 20% of $\sigma(125°)$ where the uncertainty of $\sigma(125°)$ was only 10%. This agreement demonstrates the consistency of the data.

The neutron inelastic scattering cross sections for nineteen states in ^{59}Co are shown in Figs. 10 and 11. These were obtained from the γ-ray production data by summing the contributions of γ-ray transitions which originate at a given level and subtracting the contributions of any transitions which feed the level. The inferred neutron inelastic scattering cross sections are shown as data points in Figs. 10 and 11. The solid curves are the results of theoretical calculations described below. The evaluated cross sections based on the recent (n,n') measurements of Guenther *et al.*[1] for

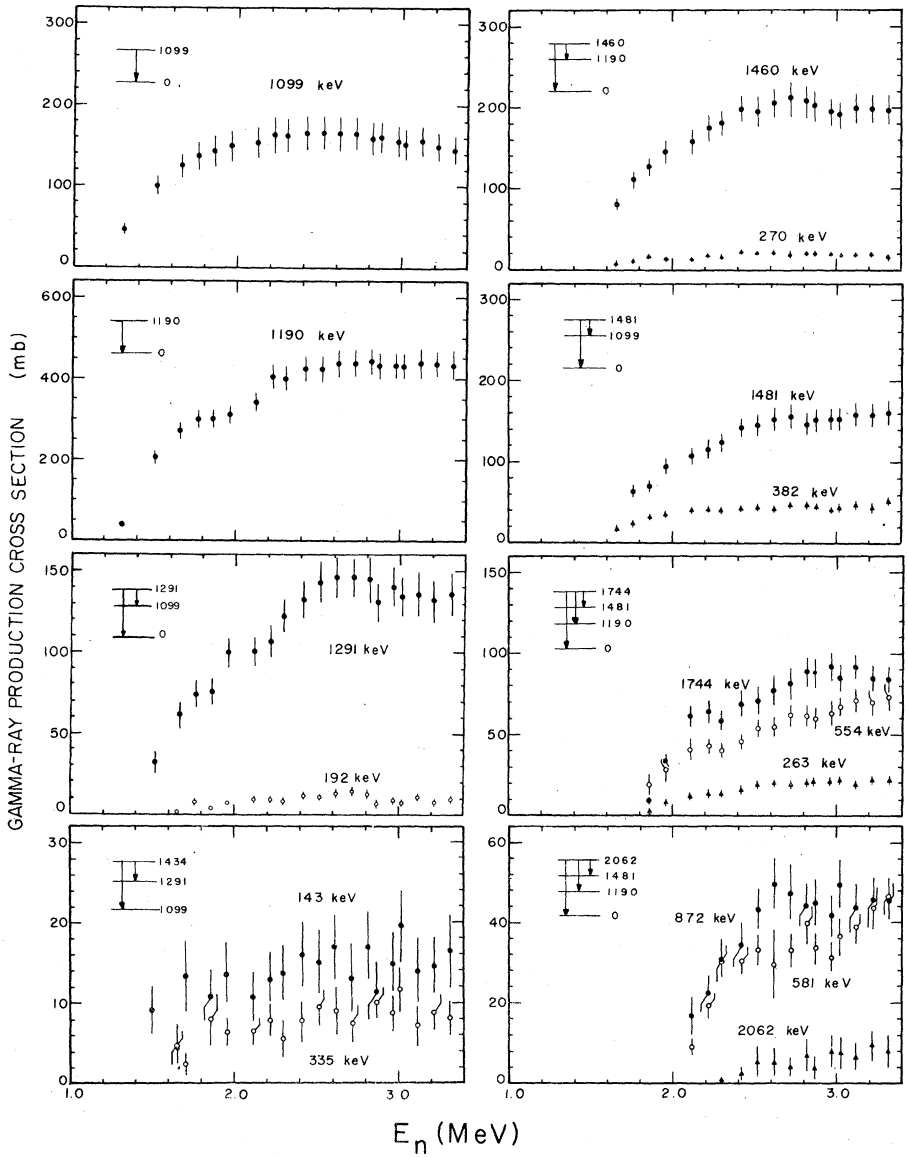

FIG. 6. ^{59}Co$(n,n'\gamma)$ integrated γ-ray production cross sections for γ rays originating from levels up to 2062 keV in excitation.

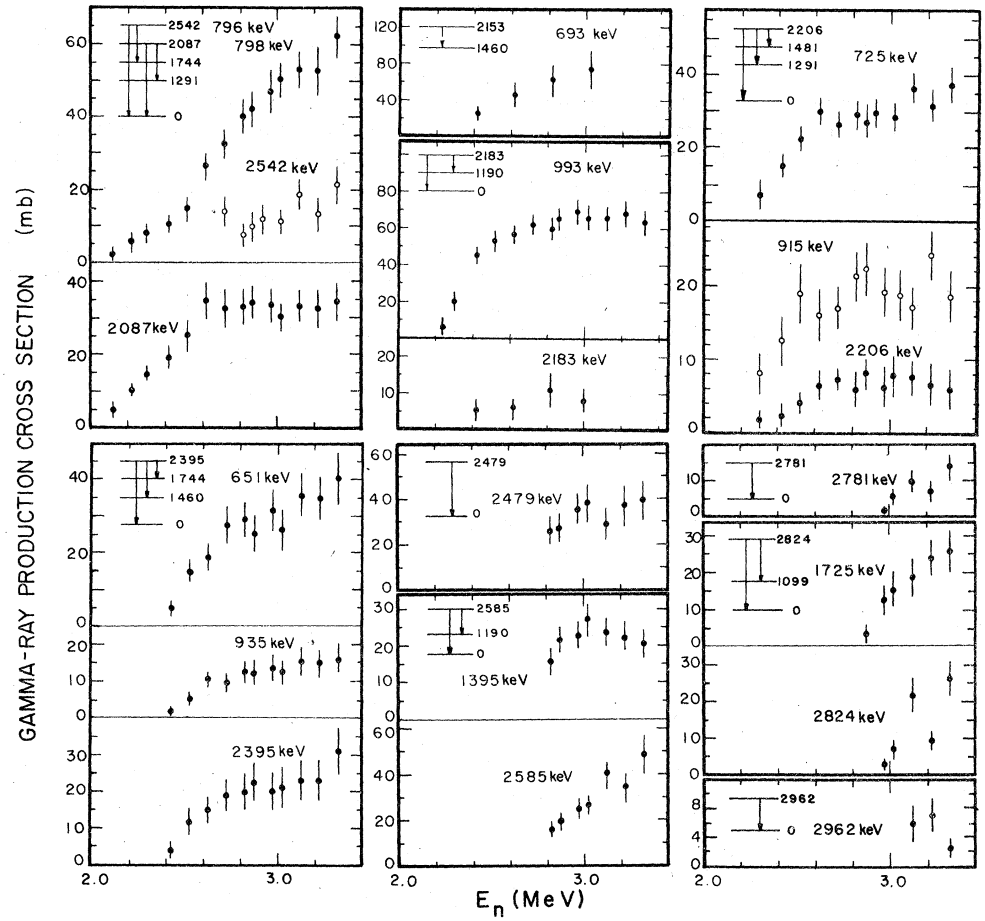

FIG. 7. $^{59}Co(n,n'\gamma)$ integrated γ-ray production cross sections for γ rays originating from levels above 2062 keV in excitation.

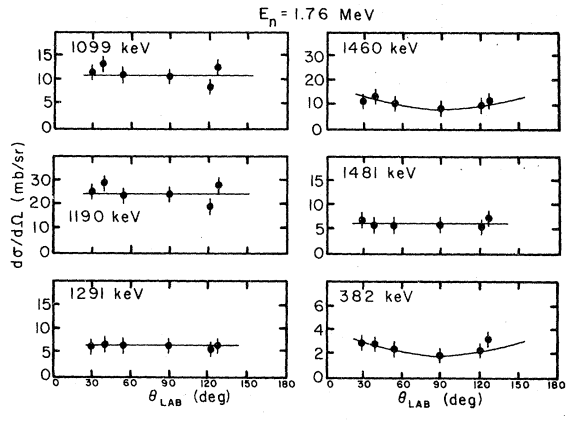

FIG. 8. Angular distributions of γ rays from ^{59}Co $(n,n'\gamma)$ at E_n=1.76 MeV. The solid curves represent Legendre polynomial fits to the data.

the 1099-, 1190-, 1291-, 1744-, and 2395-keV states are shown for comparison as dashed curves. These are also the cross sections of the ENDF/B-IV evaluation.[2]

In addition to the five individual level cross sections referred to above Guenther *et al.*[1] also report cross sections for aggregates of levels centered at 1460, 2070, 2160, and 2500 keV. These cross sections, for the five individual levels and the four composite "levels," are the only cobalt inelastic cross sections listed in ENDF/B-IV.[2]

Our data are in reasonable agreement with the work of Ref. 1 for the 1099-, 1190-, 1291-, and 1744-keV states. The agreement is especially good at energies above 2.7 MeV. Guenther *et al.*[1] report more steeply rising cross sections near threshold. This is perhaps due to extrapolation to threshold using statistical model calculations[7]

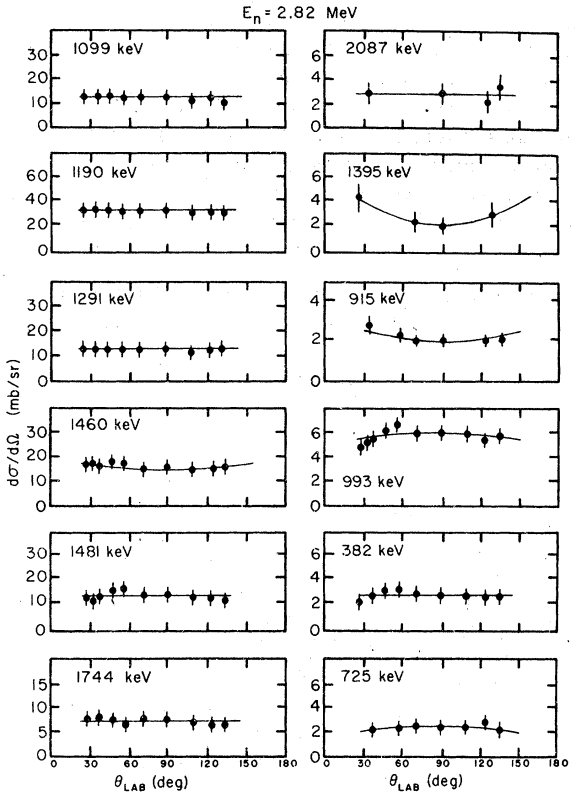

FIG. 9. Angular distributions of γ rays from ^{59}Co $(n,n'\gamma)$ at E_n = 2.82 MeV. The solid curves represent Legendre polynomial fits to the data.

which were not corrected for width fluctuation effects.[19] Our data and our calculations (described below) which incorporate width fluctuations corrections indicate less steeply rising cross sections near threshold.

The cross section for the 2395-keV level is not in agreement with Guenther *et al.*[1] Their (n,n') data indicate a level at 2350 keV which they identify with the 2395-keV state, having a cross section considerably higher than ours.

V. THEORETICAL CROSS SECTIONS

Cross sections for the excitation of a level by neutron inelastic scattering were calculated by the FORTRAN IV code MANDYF.[20] This code uses the Hauser-Feshbach[7] formalism and incorporates Moldauer's[19] width fluctuation correction procedure. As pointed out above when width fluctuation effects are neglected the calculations overestimate the cross sections near thresholds and yield more steeply rising excitation functions than the measurements indicate.

The transmission coefficients needed to calculate the inelastic scattering cross sections were obtained with the FORTRAN IV code SCAT.[21] The optical model parameters used by SCAT were obtained by a parameter search technique.[22] Initial values in this search were those of Becchetti and Greenlees.[23] The procedure involves comparing calculated and experimental differential elastic scattering cross sections and varying the initial optical model parameters until a χ^2 minimum between the calculated and experimental points is attained. This procedure was followed for eleven ^{59}Co elastic angular distributions[24] covering the energy region 0.5–4.0 MeV. The resulting points for V (the real well depth) and W (the imaginary well depth) were then least-squares fitted to obtain potential parameters. The final values of the parameters are

$$V(E) = 61.3 - 2.1E \text{ (MeV)},$$

$$W(E) = 3.94 + 1.24E \text{ (MeV)},$$

$$V_{so} = 6.4 \text{ MeV},$$

$$r_0 = 1.16 \text{ fm}, \quad r_0' = 1.22 \text{ fm}$$

$$a_0 = 0.70 \text{ fm}, \quad a_0' = 0.57 \text{ fm}.$$

The real well form factor is that of the Woods-Saxon potential. The imaginary well is a derivative Woods-Saxon type and the spin-orbit term is of the Thomas type. The somewhat unconventional energy dependence of the imaginary well yielded in addition to a best fit to the elastic data better values for the inelastic cross sections than the conventional constant term.

A comparison of the cross-section data with the theoretical calculations is useful in assigning spins. As can be seen in Figs. 10 and 11 the magnitudes of the calculated cross sections depend on the spin of the final state in a systematic way. In particular for the states of ^{59}Co in the energy region of our measurements the calculated cross section increases in magnitude as the spin is varied from $\frac{3}{2}$ to $\frac{9}{2}$. (See especially the curves shown for the 2062-keV level cross section in Fig. 10 and those for the 2781- and 2824-keV level cross sections in Fig. 11.)

VI. ANALYSIS AND INTERPRETATION

1099- and 1291-keV levels

The spin and parity of these levels are known to be $\frac{3}{2}^-$. This assignment is based upon population of levels in β-decay,[16] and upon the deduced l values of the outgoing particles in the ^{60}Ni$(t,\alpha)^{59}$Co and ^{58}Fe$(^3$He$,d)^{59}$Co reactions performed by Blair and Armstrong.[25] Additional evidence is supplied by nuclear fluorescence studies,[26] Coulomb excitation measurements employing the ^{59}Co$(^{16}$O$,^{16}$O$'\gamma)$ reaction,[27] and the ^{56}Fe$(\alpha,p\gamma)^{59}$Co work of Coop

et al.[15] Previous $(n,n'\gamma)$ studies also support these spin and parity assignments.[6,28] The large error bars at energies above 2.2 MeV are due to problems in background determination in the γ-ray spectra. All spectra had background lines near 1099 and 1291 keV. The calculations were made with the accepted $\frac{3}{2}^-$ value for J^π.

1190-keV level

The J^π of the 1190-keV level has previously been listed as $\frac{5}{2}^-$, $\frac{7}{2}^-$, or $\frac{9}{2}^-$ on the basis of the (^{16}O, ^{16}O′, γ) angular correlation measurements performed by Nordhagen *et al.*[27] with the $\frac{5}{2}^-$ assignment being the least likely. Angular correlation measurements by Coop *et al.*[15] have ruled out the $\frac{7}{2}^-$ value. The bremsstrahlung studies by Swann[26] support the $\frac{9}{2}^-$ assignment, agreeing with the spin assigned by Daniels and Felsteiner[6] on the basis of $(n,n'\gamma)$ reaction measurements and by Guenther *et al.*[1] in their (n,n') work. Our calculations give best agreement with the data for a $\frac{9}{2}^-$ spin assignment.

1434-keV level

This level is the only one below 2 MeV which does not decay directly to the ground state but

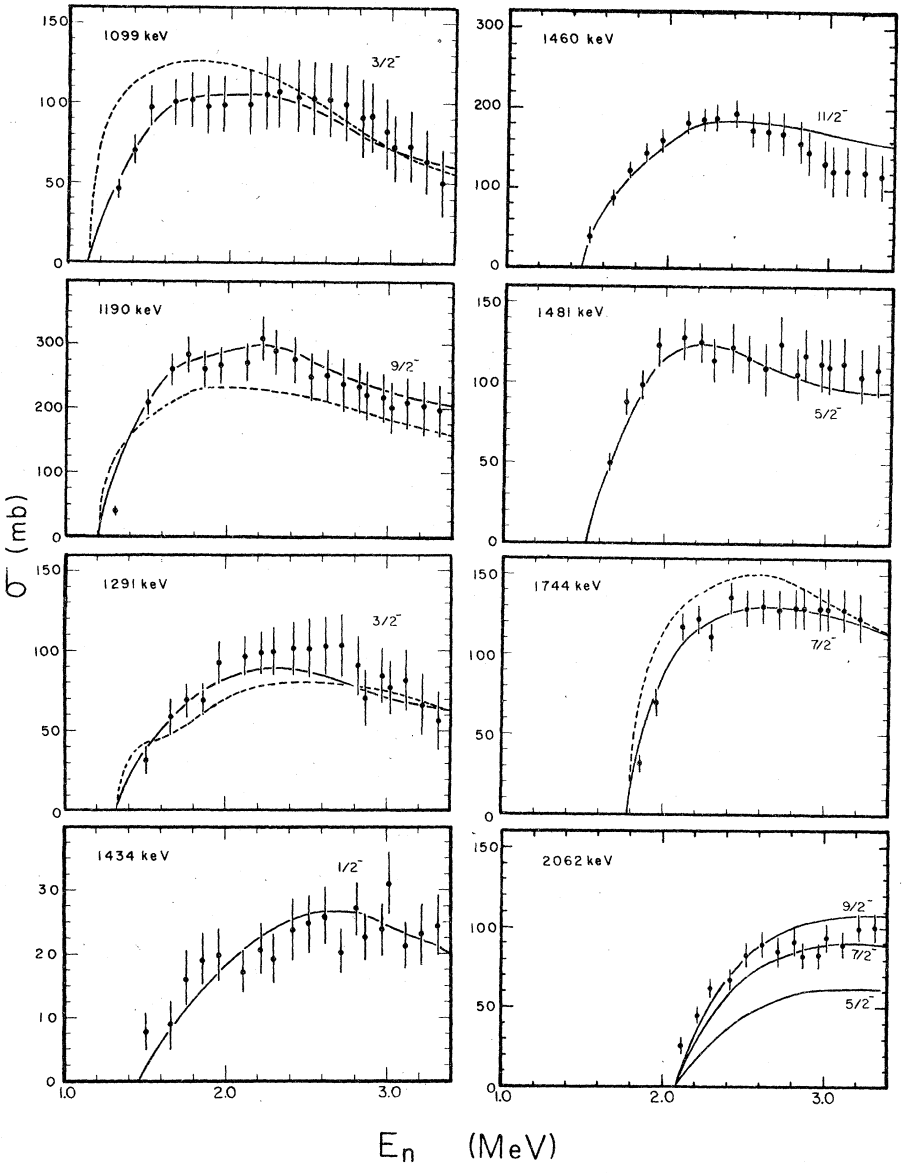

FIG. 10. Inelastic neutron scattering cross sections for ^{59}Co for levels up to 2062 keV in excitation. The solid curves represent theoretical calculations using the statistical model. The dashed curves are from the evaluation of Guenther *et al.* (Ref. 1) based on their (n,n') measurements.

rather emits two intermediate γ rays to the two $\frac{3}{2}^-$ states. β-γ coincidence[27] and γ-γ angular correlation[29] studies confirm a spin and parity of $\frac{1}{2}^-$ for this state. The relatively large (approximately 30%) errors for the experimental points, shown in Fig. 10, are the result of peak extraction errors in the 143- and 335-keV γ rays. Our results agree with the $\frac{1}{2}^-$ assignment.

1460-keV level

A variety of J^π values have previously been assigned to this level. Guenther *et al.*[1] assign $\frac{7}{2}^-$ with $\frac{9}{2}^-$ as a possible alternative. Daniels and Felsteiner[6] suggested possible values of $\frac{5}{2}^-$ and $\frac{13}{2}^-$ based upon comparison of their $(n,n'\gamma)$ data with Hauser-Feshbach calculations. Rogers *et al.*[30] have assigned a value of $\frac{5}{2}^-$ from similar considerations. Nordhagen *et al.*[27] observed the 270-keV intermediate transition between the 1460- and 1190-keV ($\frac{9}{2}^-$) levels. They assigned values of $\frac{11}{2}^-$ or $\frac{5}{2}^-$. The intermediate transition was also observed in the current work and its branching ratio determined as $9\% \pm 1\%$. The nuclear fluorescence work of Swann[26] rules out the $\frac{5}{2}^-$ value and assigns a value of $\frac{11}{2}^-$, consistent with the assignment in the present work.

This $\frac{11}{2}^-$ assignment, employed in the MANDYF calculations, yielded the correct shape for the measured angular distribution, and the correct magnitude for the excitation function. The assignment is consistent with the predictions of the unified vibrational models of Stewart *et al.*[31] and Gómez,[32] both of which indicate a spin state of $\frac{11}{2}^-$ in this energy region.

The large error bars for the data above 2.2 MeV are due to the difficulty in accounting for the feeding of the 1460-keV state by the 693-keV transition

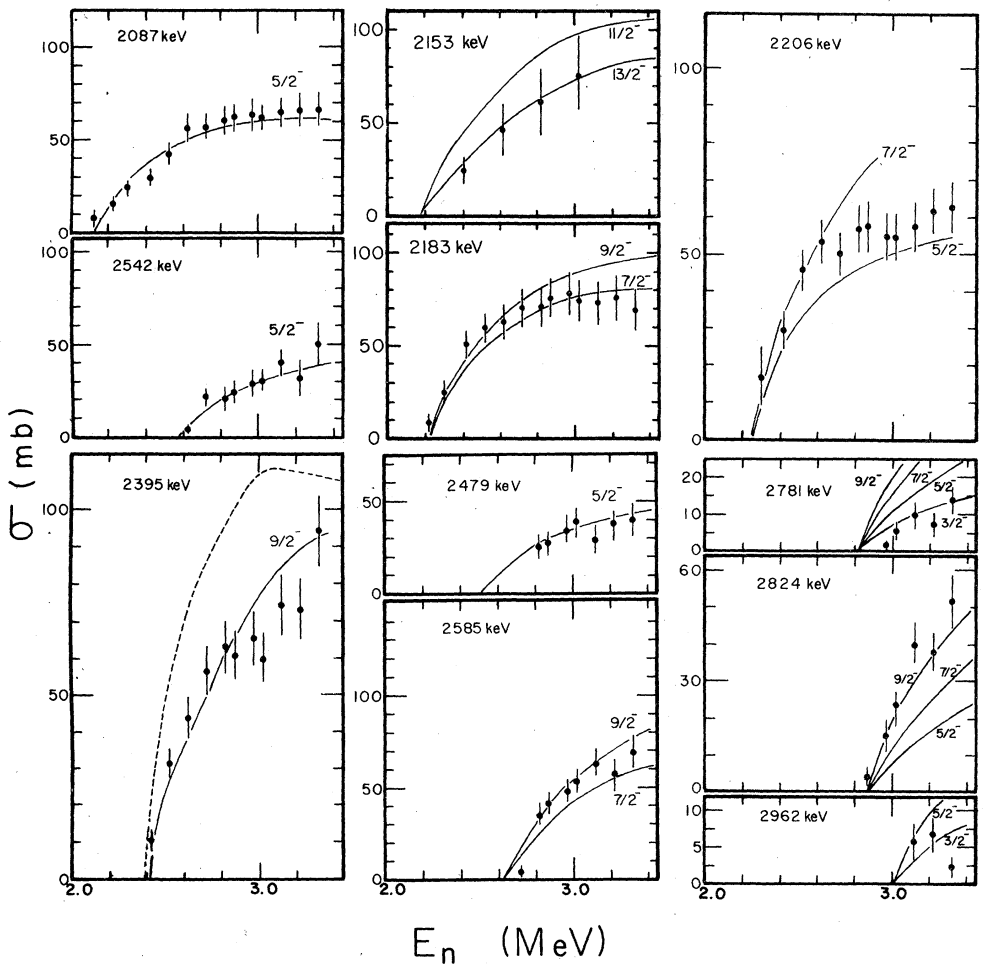

FIG. 11. Inelastic neutron scattering cross sections for ^{59}Co for levels above 2062 keV in excitation. The solid curves represent theoretical calculations using the statistical model. The dashed curve is from the evaluation of Geunther *et al.* (Ref. 1) based on their (n,n') measurements.

from the 2153-keV level. The 693-keV transition lies at the same energy as the background line due to inelastic scattering from ^{72}Ge in the detector.

1481-keV level

The Nuclear Data Sheets[16] assign a spin of $\frac{5}{2}$ to the 1481-keV state. Coop *et al.*[15] make a definite $\frac{5}{2}$ assignment on the basis of $^{56}Fe(\alpha,p\gamma)$ angular correlations. The $\frac{5}{2}$ assignment is in agreement with our calculations. No parity assignment has been made previously and the results of our calculations are generally insensitive to parity changes.

1744-keV level

This level has been studied extensively by Coop *et al.*[15] via the $^{56}Fe(\alpha,p\gamma)^{59}Co$ reaction. They assigned a J^π of $\frac{7}{2}^-$. Supporting this assignment is the $^{60}Ni(t,\alpha)^{59}Co$ work of Blair and Armstrong[25] and the Coulomb excitation work of Nordhagen *et al.*[27] The $\frac{7}{2}^-$ assignment is consistent with our results.

2062-, 2087-, and 2542-keV levels

A J^π value of $\frac{7}{2}^-$ has been assigned to the 2062-keV state by Blair and Armstrong.[25] They suggest $\frac{5}{2}^-$ for the 2087-keV state. These assignments give good agreement between our calculated and experimental cross sections. An equally good fit to our data is obtained with $\frac{9}{2}^-$ for the 2062-keV level.

There is no previous spin information on the 2542-keV state. This state decays to the $\frac{7}{2}^-$ ground state and to the $\frac{7}{2}^-$ state at 1744 keV with no decays to the $\frac{9}{2}^-$ second excited state at 1190 keV or to the 1099 keV, $\frac{3}{2}^-$ first excited state, or the $\frac{3}{2}^-$ state at 1291 keV. The best fit to our data is obtained assuming a spin of $\frac{5}{2}$ as shown in Fig. 11. In accord with the systematics in the variation of the magnitude of the calculated cross section with spin, the calculations for $\frac{7}{2}$ and $\frac{3}{2}$ (not shown) are higher and lower, respectively, than the data while a $\frac{9}{2}^-$ assignment would result in a very high cross section. We tentatively assign $\frac{3}{2}$, $\frac{5}{2}$, or $\frac{7}{2}$ to the 2542-keV state.

The 2087-keV level decays to the $\frac{7}{2}^-$, ground state (56% branch) and to the $\frac{3}{2}^-$, 1291-keV state via the 796-keV transition (44% branch). A complication arises in the yield extraction for the 796-keV γ ray above 2.6-MeV bombarding energy because the 2542-keV level decays by a 798-keV transition to the 1744-keV state. It was impossible to resolve these two transitions in the spectra so the combined γ-ray production cross sections are shown in Fig. 7. Since the branching ratios for the 796-keV and 2087-keV transitions were known from data taken below the threshold for the 798-keV transition, it was possible to separate out the 796-keV contribution from the combination.

Coop *et al.*[15] observed the 798-keV branch from the 2542-keV state but assigned it an 80% branching ratio. Presumably their large value was due to the inclusion of the 796-keV transition from the 2087-keV state. They also report transitions from the 2087-keV state to the ground state and to the 1099-keV state, but no 796-keV line. The transition of 988 keV (2087 → 1099) was not observed in the present experiment.

Brondi *et al.*[18] observed the 976-keV transition from the 2087-keV level but the 2542-keV state was not excited at all in the γ decay of the analog of the ^{56}Fe ground state which they studied.

2153-keV level

This state decays only via the 693-keV transition to the $\frac{11}{2}^-$ state at 1460-keV suggesting that it may be an $\frac{11}{2}$ or $\frac{13}{2}$ state. Although our data have large errors (±30%) due to the 693-keV background line, we are able to obtain good agreement with the theory for a $\frac{13}{2}^-$ assignment. Transitions to the $\frac{9}{2}$ state at 1190-keV or to the $\frac{7}{2}$ ground state, which might be expected for a $\frac{7}{2}$, $\frac{9}{2}$, or $\frac{11}{2}$ assignment, were not observed. A $\frac{15}{2}$ assignment, while not eliminated by the selection rules, is unlikely since it would yield a cross-section value which is too small.

2183-keV level

This level decays to the $\frac{7}{2}^-$ ground state and to the $\frac{9}{2}^-$ state at 1190 keV via a strong 993-keV transition. The ground state transition has not been observed previously. Our results suggest a $\frac{7}{2}^-$ or $\frac{9}{2}^-$ assignment on the basis of comparison of Hauser-Feshbach calculations to the data. Figure 11 shows the calculations for both $\frac{9}{2}^-$ and $\frac{7}{2}^-$ with the latter value yielding a better fit to the data.

2206- and 2395-keV levels

A tentative spin assignment of $\frac{3}{2}$, $\frac{5}{2}$, or $\frac{7}{2}$ has been made for the 2206-keV level. Calculations for both $\frac{7}{2}^-$ and $\frac{5}{2}^-$ are shown in Fig. 11 with the $\frac{5}{2}^-$ assignment giving the best representation of the data.

The 2395-keV state has been observed in $(p,p'\gamma)$ reactions[33] and in neutron scattering studies.[1] A tentative assignment of $\frac{9}{2}^-$ was made in the latter work. Our data agree well with theory for the $\frac{9}{2}^-$ assignment. Tentatively we assign $\frac{7}{2}$, $\frac{9}{2}$, or $\frac{11}{2}$.

2479-keV level

Our results favor a spin of $\frac{5}{2}$ for this level. The decay is to the ground state. Figure 11 shows that

the calculation for $\frac{5}{2}$ agrees very well with the data. A $\frac{7}{2}$ or $\frac{3}{2}$ assignment would yield higher and lower theoretical cross sections consistent with the systematics mentioned above. No transitions are observed to the $\frac{3}{2}^-$ states at 1099 or 1291-keV, nor to the $\frac{7}{2}^-$ state at 1744 keV. Tentatively we assign $\frac{3}{2}$, $\frac{5}{2}$, or $\frac{7}{2}$.

2585-keV level

The 2585-keV level has been observed by Blair and Armstrong[25] in their ^{60}Ni(t, ^{4}He)^{59}Co work. Their angular distribution analysis of the emitted α's suggests a J^π value of $\frac{7}{2}^-$. Our results are not inconsistent with that assignment but we obtained a somewhat better fit assuming $\frac{9}{2}^-$.

2713- and 2781-keV levels

The 2713-keV state is very weakly excited in this experiment and it decays via a 1614-keV transition to the $\frac{3}{2}^-$ state at 1099 keV. Blair and Armstrong[25] observed this state and suggest a J^π of $\frac{1}{2}^+$. This is consistent with statistical model calculations which yield very small cross sections for $\frac{1}{2}$ or $\frac{3}{2}$ assignments. Shell model predictions[31,32] do indicate some low spin states in this region of excitation and this is a likely candidate. No cross-section information was extracted for this state.

The 2781-keV state was weakly excited in the experiment. Only a ground state transition was observed. The magnitude of the cross section agrees with a $\frac{3}{2}^-$ ($E2$) transition. Calculations for $\frac{5}{2}^-$, $\frac{7}{2}^-$, and $\frac{9}{2}^-$ give results which are too high. We assign $\frac{3}{2}^-$ or $\frac{5}{2}^-$.

2816- and 2824-keV levels

Evidence for the 2816-keV level, which is not reported in the Nuclear Data Sheets[16] but was reported by Brondi *et al.*,[18] who observed the ground state transition, is based on the observation of the 2816-keV transition in one spectrum, viz., the 3.5-MeV spectrum shown in Fig. 4. The state at 2824 keV was observed to decay via strong transitions to the $\frac{7}{2}^-$ ground state and the $\frac{3}{2}^-$ first excited state at 1099 keV. In addition a weak branch was observed to the $\frac{9}{2}^-$ second excited state at 1190 keV. Best agreement between theory and experiment is obtained assuming $\frac{9}{2}$ for the spin of the 2824-keV state. This is the only case where the spin which yields the best fit to the experimental cross section is inconsistent with the most likely spins based on branching ratio information. The selection rules make it unlikely that a $\frac{9}{2}$ state would decay strongly to a $\frac{3}{2}$ state.

Blair and Armstrong[25] observed a state at 2818 keV to which they assigned a tentative J^π of $\frac{3}{2}^-$. It is not clear which member of the doublet they observed. Mateja *et al.*[17] reported this doublet at 2820 and 2829 keV. Perhaps the contribution from the state at 2816 keV has been inadvertently included in our 2824-keV ground state transition and is responsible for its apparent strength. From our results we can only assign a range of values $\frac{3}{2}-\frac{9}{2}$ for the 2824-keV state.

2962- and 3016-keV levels

The 2962-keV state decays to the ground state. This was the highest energy transition observed in the present work. Calculations shown in Fig. 11 are for $\frac{3}{2}^-$ and $\frac{5}{2}^-$. Only a ground state transition was observed and no transition to the $\frac{3}{2}^-$ states at 1099 and 1291 keV. The large error bars on the data for this state reflect the low γ-ray yield. Tentatively we assign $\frac{3}{2}$, $\frac{5}{2}$, or $\frac{7}{2}$.

A transition of 1553 keV appears in our high energy spectra. It is likely to originate at the 3016-keV state reported in the work of Mateja *et al.*[17] No cross-section information has been extracted for this state. The decay of the 3016-keV state to the 1460-keV, $\frac{11}{2}^-$ state via the 1553-keV transition and the absence of any other branches suggests that the 3016-keV level is possibly a high spin state ($\frac{11}{2}$ or $\frac{13}{2}$).

VII. COMPARISON WITH MODEL CALCULATIONS

Figure 12 shows a comparison of the energy level scheme with spin information obtained in this work to the unified vibrational model calculations of Stewart *et al.*[31] and Gómez.[32] These calculations represent the best theoretical attempts at accounting for the structure of ^{59}Co. We show the parities of the states as negative in our experimental results. We are not able to make definitive parity determinations in our work and therefore our parity assignments simply reflect the theoretically predicted preponderance of negative parity states in this region of excitation.

The intermediate coupling calculations of Stewart *et al.*,[31] which are based on a version of the unified vibrational model and incorporate both anharmonic core vibrations as well as quasiparticle effects, give the better representation of the level structure with respect to energies, number of levels, spacings, and spin. The theory accounts for all of the observed levels below 2.0 MeV. The ($\frac{11}{2}^-$, $\frac{13}{2}^-$) state, observed at 2153 keV, is the first experimental indication of a high spin state above 2 MeV. Both theories predict a high spin state between 2 and 3 MeV ($\frac{11}{2}^-$ for Gómez[32] and $\frac{13}{2}^-$ for Stewart *et al.*[31] but at higher energies than 2153 keV. Both theories predict a $\frac{1}{2}^-$ state between 2

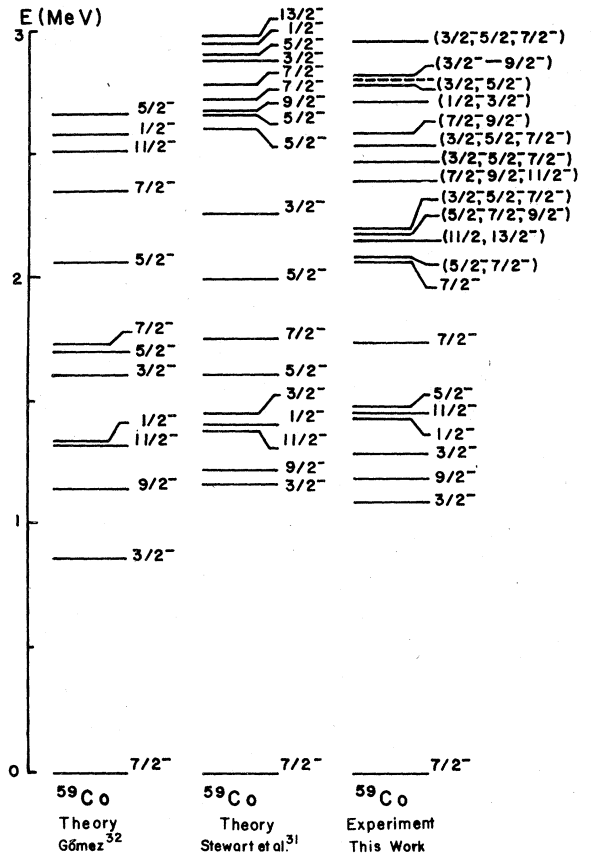

FIG. 12. A comparison of the ^{59}Co energy level scheme with spin assignments of the present work to the unified vibrational model calculations of Stewart *et al.* (Ref. 31) and Gómez (Ref. 32).

and 3 MeV and the 2713-keV level appears to be the most likely candidate.

VIII. SUMMARY AND CONCLUSION

The present work is a detailed study of the ^{59}Co neutron inelastic cross section. Much of this work represents the only available data on individual level cross sections to date, especially above 2 MeV in excitation. ENDF/B-IV lists individual level cross sections for only five states 1099, 1190, 1291, 1744, and 2395 keV. The present work reports cross sections for individual levels for these five states plus an additional fourteen levels at 1434, 1460, 1481, 2062, 2087, 2153, 2183, 2206, 2479, 2542, 2585, 2781, 2824, and 2962 keV.

The cross-section measurements are useful as an aid in establishing the spins of the levels. The magnitude of the calculated excitation functions are sensitive to spin changes, and a comparison of the cross-section data with theory coupled with the branching ratio and decay data yields considerable spectroscopic information. The γ-ray angular distributions, for the most part, are nearly isotropic and are not a sensitive test of spin assignments. They are, however, necessary in order to accurately establish the neutron cross sections for the levels. The Hauser-Feshbach theory, employing optical model transmission coefficients derived from a potential which gives a best fit to ^{59}Co elastic data, agrees remarkably well with the data (even in absolute magnitude) for levels at all excitation energies over the entire bombarding energy region.

ACKNOWLEDGMENTS

The authors are grateful to Dr. E. Sheldon, Dr. M. A. Doyle, and Dr. D. R. Donati for assistance in the preparation of the computer codes. We acknowledge Dr. B. K. Barnes, Dr. D. J. Pullen, Dr. P. Harihar, Dr. J. A. Correia, and Mr. C. E. Connolly and Ms. N. B. Sullivan for their assistance during the many hours of data taking. This work was supported in part by the National Science Foundation.

[1]P. T. Guenther, P. A. Moldauer, A. B. Smith, D. L. Smith, and J. F. Whalen, Report No. ANL/NDM-1, Argonne National Laboratory, 1973 (unpublished); P. T. Guenther, P. A. Moldauer, A. B. Smith, and J. F. Whalen, Nucl. Sci. Eng. 54, 273 (1974).

[2]Evaluated Nuclear Data File-B (ENDF/B MAT 1199), evaluation by T. Krieger, A. B. Smith, and D. Smith, National Neutron Cross Section Center, 1975 (unpublished).

[3]V. E. Scherrer, B. A. Allison, and W. R. Faust, Phys. Rev. 96, 386 (1954).

[4]S. C. Mathur, P. S. Buchanan, W. E. Tucker, D. O. Nellis, and I. L. Morgan, Texas Nuclear Corporation Report No. ORO-2791-32, 1971 (unpublished).

[5]D. L. Broder, A. F. Gamaly, A. I. Lashuk, and I. P. Sadokhin, *Second International Conference on Nuclear Data for Reactors* (International Atomic Energy Agency, Vienna, 1971), Vol. II, p. 295.

[6]J. M. Daniels and J. Felsteiner, Can. J. Phys. 46, 1849 (1968).

[7]W. Hauser and H. Feshbach, Phys. Rev. 87, 336 (1952).

[8]J. J. Egan, G. H. R. Kegel, G. P. Couchell, A. Mittler, B. K. Barnes, W. A. Schier, D. J. Pullen, P. Harihar, T. V. Marcella, N. B. Sullivan, E. Sheldon, and A. Prince, in *Nuclear Cross Sections and Technology, Proceedings of a Conference*, edited by R. A. Schrack and C. D. Bowman (National Bureau of Standards Special Publication 425, Washington, D.C., 1975).

[9]W. D. Allen, in *Fast Neutron Physics Part I,* edited by J. B. Marion and J. L. Fowler (McGraw-Hill, New York, 1960); A. D. Hanson and J. L. McKibben, Phys. Rev. 72, 673 (1947).
[10]S. J. Bame, E. Haddad, J. E. Perry, and R. S. Smith, Rev. Sci. Instrum. 28, 997 (1957).
[11]C. H. Johnson, in *Fast Neutron Physics Part I,* edited by J. B. Marion and J. L. Fowler (McGraw-Hill, New York, 1960).
[12]D. R. Donati and S. C. Mathur, Proceedings of the DECUS Spring Symposium No. 41, 1970 (unpublished).
[13]W. E. Kinney, Nucl. Instrum. Methods 83, 15 (1970).
[14]V. C. Rogers and A. Mittler, Trans. Am. Nucl. Soc. 15, 532 (1972).
[15]K. L. Coop, I. G. Graham, and E. W. Titterton, Nucl. Phys. A150, 346 (1970).
[16]Nucl. Data Sheets 17, 485 (1976).
[17]J. F. Mateja, J. A. Bieszk, J. T. Meek, J. D. Goss, A. A. Rollefson, P. L. Jolivette, and C. P. Browne, Phys. Rev. 13, 2269 (1976).
[18]A. Brondi, R. Moro, P. Pelfer, and F. Terrasi, Nuovo Cimento 30, 483 (1975).
[19]P. A. Moldauer, Rev. Mod. Phys. 36, 1079 (1964).
[20]E. Sheldon and R. M. Strang, Comp. Phys. Commun. 1, 35 (1969); E. Sheldon, S. Mathur, and D. Donati, *ibid.* 2, 272 (1971); E. Sheldon, S. Mathur, and D. Donati, *ibid.* 5, 304 (1973).
[21]W. R. Smith, Comp. Phys. Commun. 1, 106 (1969).
[22]F. G. Perey, Phys. Rev. 131, 745 (1963).
[23]F. D. Becchetti and G. W. Greenlees, Phys. Rev. 182, 1190 (1969).
[24]Data obtained from National Neutron Cross Section Center, Brookhaven National Laboratory; S. C. Gorlov, Dokl. Ak. Nauk. 158, 594 (1964), translation in Sov. Phys. Dokl. 9, 806 (1965); S. A. Cox, Bull. Am. Phys. Soc. 10, 576 (1965); F. G. Perey, *ibid.* 12, 512 (1967).
[25]A. G. Blair and D. D. Armstrong, Phys. Rev. 151, 930 (1966); Phys. Rev. 140, B1567 (1965).
[26]C. P. Swann, Nucl. Phys. A172, 569 (1971).
[27]R. Nordhagen, B. Elbek, and B. Herskind, Nucl. Phys. A104, 353 (1967).
[28]S. C. Mathur, W. E. Tucker, and I. L. Morgan, Bull. Am. Phys. Soc. 10, 577 (1965).
[29]I. Arens and H. J. Korner, Z. Phys. 242, 138 (1971).
[30]V. C. Rogers, S. C. Mathur, and P. S. Buchanan, Bull. Am. Phys. Soc. 14, 852 (1969).
[31]K. W. C. Stewart, B. Castel, and B. P. Singh, Phys. Rev. C 4, 2131 (1971).
[32]J. M. G. Gómez, Phys. Rev. C 6, 149 (1972).
[33]A. A. Katsonos, J. R. Huizenga, and H. K. Vonach, Phys. Rev. 141, 1053 (1966).